

# Post-cyclic Behavior of Compacted Clay-sand Mixtures

Hossein Soltani-Jigheh<sup>1</sup>, Abbas Soroush<sup>2</sup>

<sup>1</sup>PhD Student of Geotechnical Engineering, Dept. of Civil and Environmental Engineering, Amirkabir University of Technology, Tehran, Iran, E-mail: hsoltani@aut.ac.ir

<sup>2</sup>Associate Professor, Dept. of Civil and Environmental Engineering, Amirkabir University of Technology, Tehran, Iran, E-mail: Soroush@aut.ac.ir

*Abstract: This paper presents the results of a series of monotonic and post-cyclic triaxial tests carried out on a clay specimen and three types of clay-sand mixed specimens. The focus of the paper is on the post-cyclic mechanical behavior of the mixed specimens, as compared to their monotonic behavior. Analyses of the tests results show that cyclic loading degrade undrained shear strength and deformation modulus of the specimens during the post-cyclic monotonic loading. The degradation depends on the sand content, the cyclic strain level and to some degrees to the consolidation pressure.*

*Keywords: mixed clayey soils, undrained behavior, triaxial testing, post-cyclic loading, pore water pressure*

## 1. Introduction

Materials of earth dams, glacial tills, mudflows, debris flows, and residual and colluvial soil deposits have a distinct structure. These materials consist of a mixture of large particles (gravel, sand or hard clay fragments) and a soft matrix of soil (clay, or silt-clay mixture). These types of soils are called "mixed or intermediate soils". When the clay content is dominant in the mixed soil, it is called mixed clayey soil. The behavior of such soils depends on the amount of granular material and clay content as well. Over the past decades, the behavior of mixed clayey soils under monotonic and cyclic loading has been studied to some extent [1, 2, 3, 4, 5, 6, 7 and 8].

In order to perform the stress-strain and stability analyses of a soil structure made of clay-granular material mixtures, their mechanical properties are required. It is common practice to design soil structures, like earth and rockfill dams to withstand both

static and dynamic loading (e.g. earthquake shaking). However, a review on the performance of earth dams during earthquakes shows that most of the dam failures have occurred either a few hours or up to 24 hours after the earthquake. This phenomenon is called *delayed failure* or *delayed response*, and means that the critical period for an earth dam is not only the period of shaking, but also a period of hours following the earthquake. It therefore necessitates the investigation of post-earthquake behavior of such structures [9, 10, 11, 12, 13, 14 and 15]. Hence, it is of great importance to understand post-earthquake behavior of comprising material of these structures. Published data show that a number of post-cyclic monotonic shear tests have been carried out on clayey soils [16, 17, 18, 19, 20 and 21], and the post-liquefaction behavior of sandy and silty soils has also been studied extensively [22, 23, 24, 25, 26, 27 and 28]; however, the post-cyclic behavior of mixed clayey soils has never been studied.

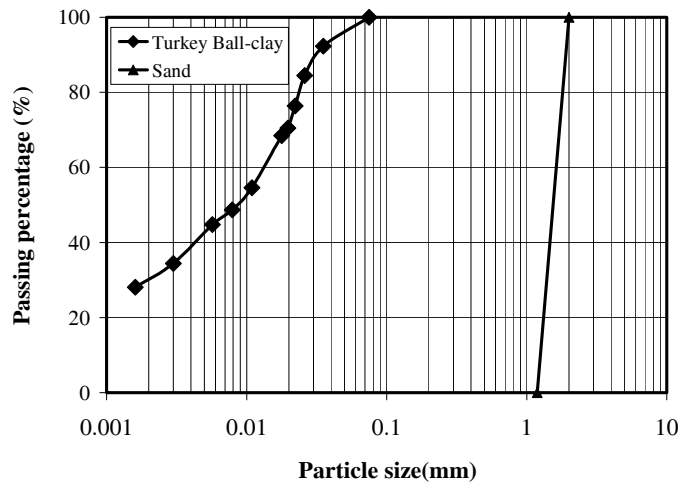


Figure 1. Grain size distributions of tested materials

This paper focuses mainly to understand the behavior of artificially mixed clays with sands subjected to post-cyclic monotonic loading. For this purpose, a laboratory study program was set to investigate the effect of cyclic loading, sand content, and consolidation pressure on post-cyclic mechanical behavior of mixed clayey soils.

## 2. Testing Procedure

### 2.1. Apparatus and Materials

The testing apparatus was a closed-loop digitally servo-controlled apparatus capable of performing static and dynamic triaxial tests. Four types of reconstituted compacted soil specimens were tested. Three types of the specimens were clay-sand mixtures and the other one was pure clay. Commercial clay, Turkey Ball-clay, was used to minimize the risk of plasticity variations. The index properties of the clay were  $LL=41$ ,  $PI=18$ , and  $G_s=2.72$ . According to the Unified Soil Classification System (USCS), the clay is categorized as CL [29]. The sand used in the

mixtures was retrieved from the Khalij area in the vicinity of Tehran and comprised subrounded aggregates with  $G_s=2.64$ . The grain size distributions of the clay and sand are presented in Figure 1.

The clay-sand specimens were prepared by mixing different volumetric proportions of the clay and sand and named ST80, ST60 and ST40, where S and T stand for the sand and clay, respectively and the numbers denote the volumetric clay percentage; the specimen made of pure clay named T100.

### 2.2. Specimens Preparation

Since the main purpose of the research was to evaluate the behavior of mixed clayey soils as materials for the core of earth dams, the specimen preparation method was chosen so to model the prototype conditions as much as possible. Each of the specimens was compacted in six layers with a water content of 2% wet of optimum and its corresponding dry density according to the standard compaction test [29]. Table 1 presents the dry

Table 1. Dry density and water content of the specimens

| Specimen | $\gamma_d$ (kN/m <sup>3</sup> ) | w (%) |
|----------|---------------------------------|-------|
| T100     | 15.90                           | 23.90 |
| ST80     | 16.60                           | 18.33 |
| ST60     | 16.95                           | 16.93 |
| ST40     | 18.10                           | 15.26 |

density and water content of the specimens before testing. The specimens were 7.1cm in diameter and 15cm in height.

To attain homogenous specimens, materials (clay and sand) needed for each of the layers were mixed with water separately and kept isolated in a plastic bag for about 24 hours before the compaction. The surface of each layer was scored after compaction for better binding with the next layer.

### 2.3. Consolidation and Shearing

The prepared specimens were mounted in the triaxial cell and carbon dioxide gas was then flushed through them from the bottom to the top to displace all the entrapped air out of the specimens. Water was then let flow through the specimens and back-pressures were applied until a saturation degree corresponding to B-value of 96% was achieved. Then specimens were consolidated isotropically under effective confining pressures ( $\sigma'_c$ ) of 100, 200 and 350kPa.

Two series of undrained shear tests were carried out on the specimens; Series I: conventional monotonic compression shearing and Series II: cyclic undrained loading followed by monotonic compression shearing. Series I tests were carried out to provide bases for the comparison and evaluation of the results of the post-cyclic

monotonic tests. Sufficient numbers of repeatability tests was carried out that their results were conforming. The loading for all of the cyclic tests was strain-controlled, which is preferred usually over the stress-controlled loading for cyclic loading tests [30]. The monotonic loading (Series I and post-cyclic shearing of Series II tests) were conducted with a constant strain rate of 0.08 % / min up to an axial strain of 16%.

In Series II tests, the specimens were subjected first to 50 cycles of constant cyclic axial strain amplitude ( $\varepsilon_c$ ) with frequency of 0.1Hz. Then enough time was given for equalization of residual excess pore water pressures, before the post-cyclic monotonic compression shearing was applied. In order to investigate effects of different cyclic loading amplitudes on the post-cyclic behavior of the specimens, almost all of the cyclic tests were repeated with three cyclic axial strains. The loading processes applied to each of the specimens for Series I and II tests are schematically illustrated in Figure 2.

### 3. Tests Results

Typical results of the undrained monotonic and post-cyclic monotonic tests on the T100, ST80, ST60 and ST40 specimens are presented in Figures 3 to 6, respectively. There are four curves in every graph, one for

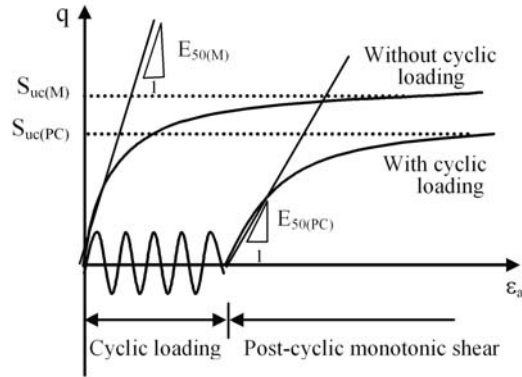


Figure 2. Loading processes applied to the specimens

Table 2. Mean effective stresses ( $p'_{pc}$ ) and apparent overconsolidation ratios ( $OCR_{app}$ )\* at the beginning of post-cyclic tests

| Consolidation Pressure | $\sigma'_c=100\text{kPa}$ |                       | $\sigma'_c=200\text{kPa}$ |                       |                       | $\sigma'_c=350\text{kPa}$ |                       |                       |
|------------------------|---------------------------|-----------------------|---------------------------|-----------------------|-----------------------|---------------------------|-----------------------|-----------------------|
|                        | $\varepsilon_c=0.25\%$    | $\varepsilon_c=0.5\%$ | $\varepsilon_c=0.5\%$     | $\varepsilon_c=1.0\%$ | $\varepsilon_c=1.5\%$ | $\varepsilon_c=0.5\%$     | $\varepsilon_c=1.0\%$ | $\varepsilon_c=1.5\%$ |
| T100                   | 80 (1.25)                 | 67.8 (1.47)           | 138.8 (1.44)              | 126 (1.59)            | 83 (2.41)             | 240 (1.46)                | 187.5 (1.87)          | 178 (1.97)            |
| ST80                   | 70(1.43)                  | 54 (1.85)             | 96.5 (2.07)               | 82 (2.44)             | 74 (2.7)              | 256.7 (1.36)              | 172.4 (2.03)          | 164.7 (2.13)          |
| ST60                   | 77 (1.3)                  | 40.4 (2.48)           | 117.5 (1.7)               | 111 (1.8)             | 101 (1.98)            | 195 (1.79)                | 118.5 (2.95)          | 96 (3.65)             |
| ST40                   | 48 (2.1)                  | 32.3 (3.1)            | 97 (2.06)                 | 69 (2.9)              | 59.5 (3.36)           | 156 (2.24)                | 99 (3.54)             | 83.5 (4.19)           |

\* Numbers inside parentheses introduce ( $OCR_{app}$ ) apparent overconsolidation ratio

the monotonic test and the others for the post-cyclic monotonic tests. Each of the figures includes variations of deviatoric stress versus axial strain, excess pore water pressure versus axial strain and deviatoric stress versus mean normal effective stress. For the purpose of brevity, only the immediate results of the tests with  $\sigma'_c=200\text{kPa}$  are presented here. Nevertheless, the results of all of the tests with  $\sigma'_c=100, 200, \text{ and } 350\text{kPa}$  are included in the analyses and discussions which will be presented in the next section.

It should be noted that  $\sigma'_c$  is the consolidation pressure before shearing in Series I tests and before cyclic loading in

series II tests. Therefore, it should not be taken wrongly as the mean effective stress ( $p'_{pc}$ ) at the beginning of post-cyclic monotonic shearing, which is considerably lower than its corresponding  $\sigma'_c$ . The mean effective stresses and their associated apparent overconsolidation ratios ( $OCR_{app}$ ) before post-cyclic shearing are tabulated in Table 2. The apparent overconsolidation ratio is defined as  $\sigma'_c / p'_{pc}$ .

Results of the cyclic tests were found to be in general agreement with the results of similar tests reported in the literature [1, 3, 5, 7 and 8]. The cyclic tests results and their evaluation are out of the scope of this paper and therefore, they are not presented here.

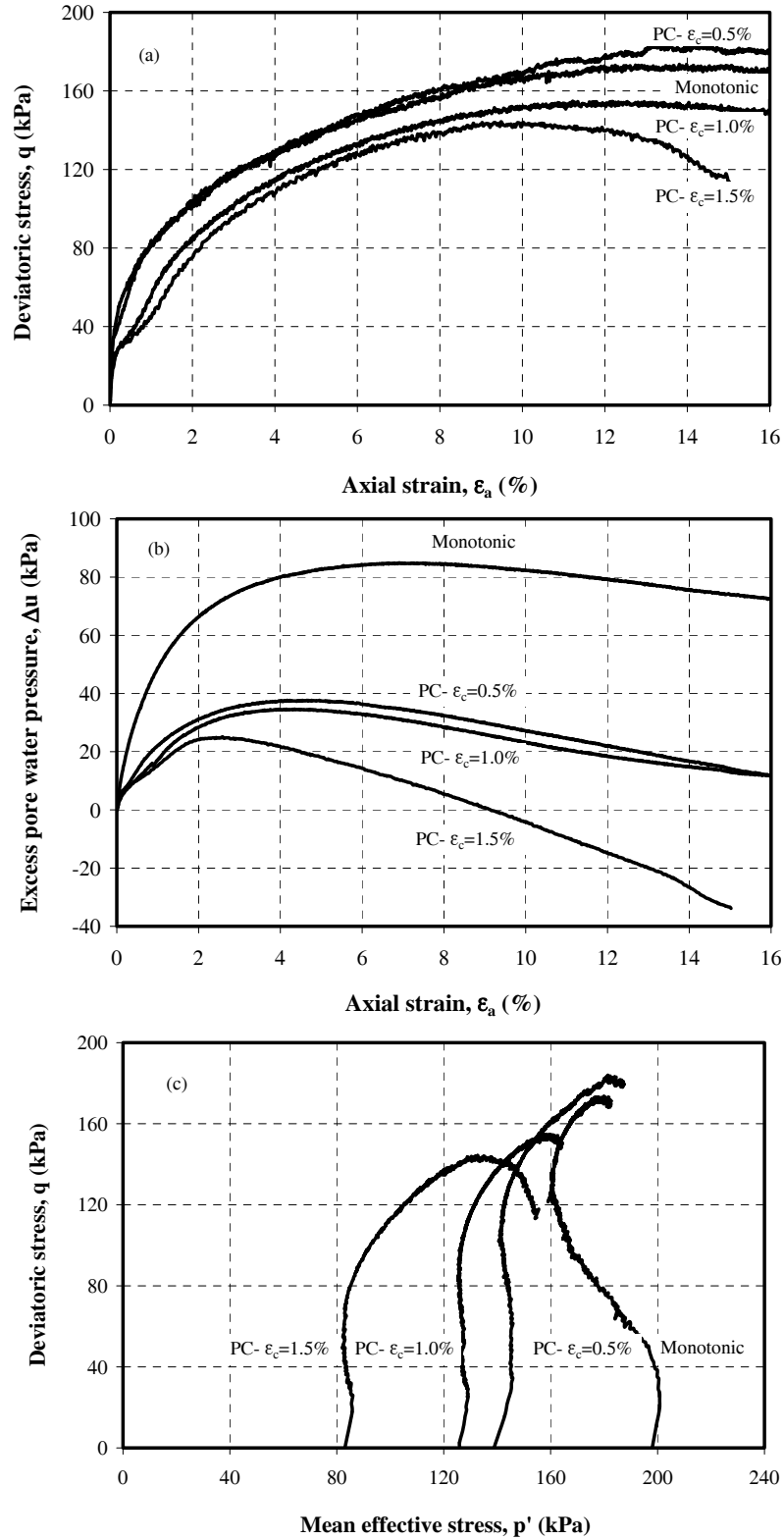


Figure 3. Effect of cyclic loading on post-cyclic behavior of specimen T100 at  $\sigma'_c=200$ kPa: a) deviatoric stress versus axial strain, b) excess pore water pressure versus axial strain and c) effective stress path

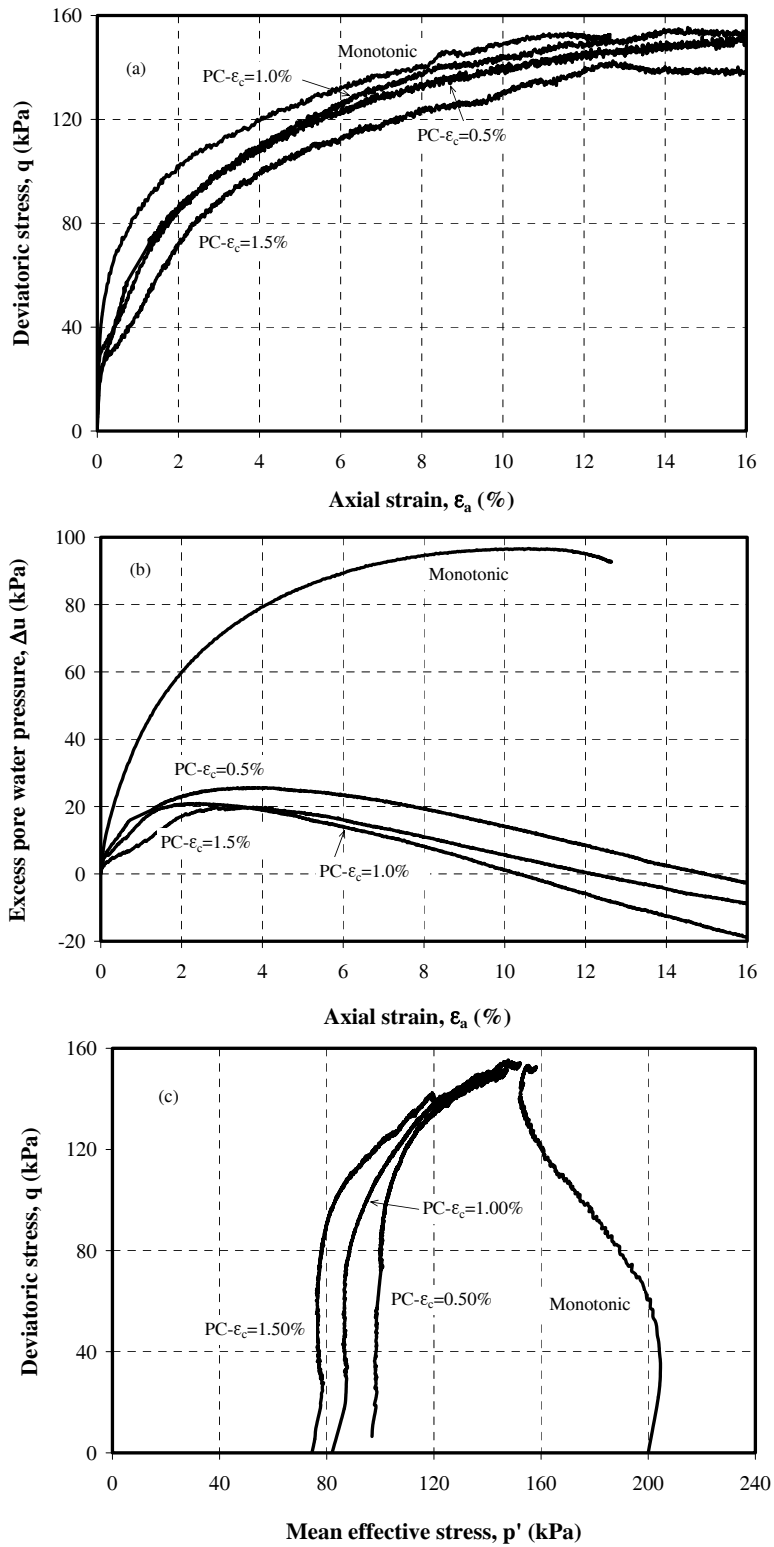


Figure 4. Effect of cyclic loading on post-cyclic behavior of specimen ST80 at  $\sigma'_c = 200$  kPa: a) deviatoric stress versus axial strain, b) excess pore water pressure versus axial strain and c) effective stress path

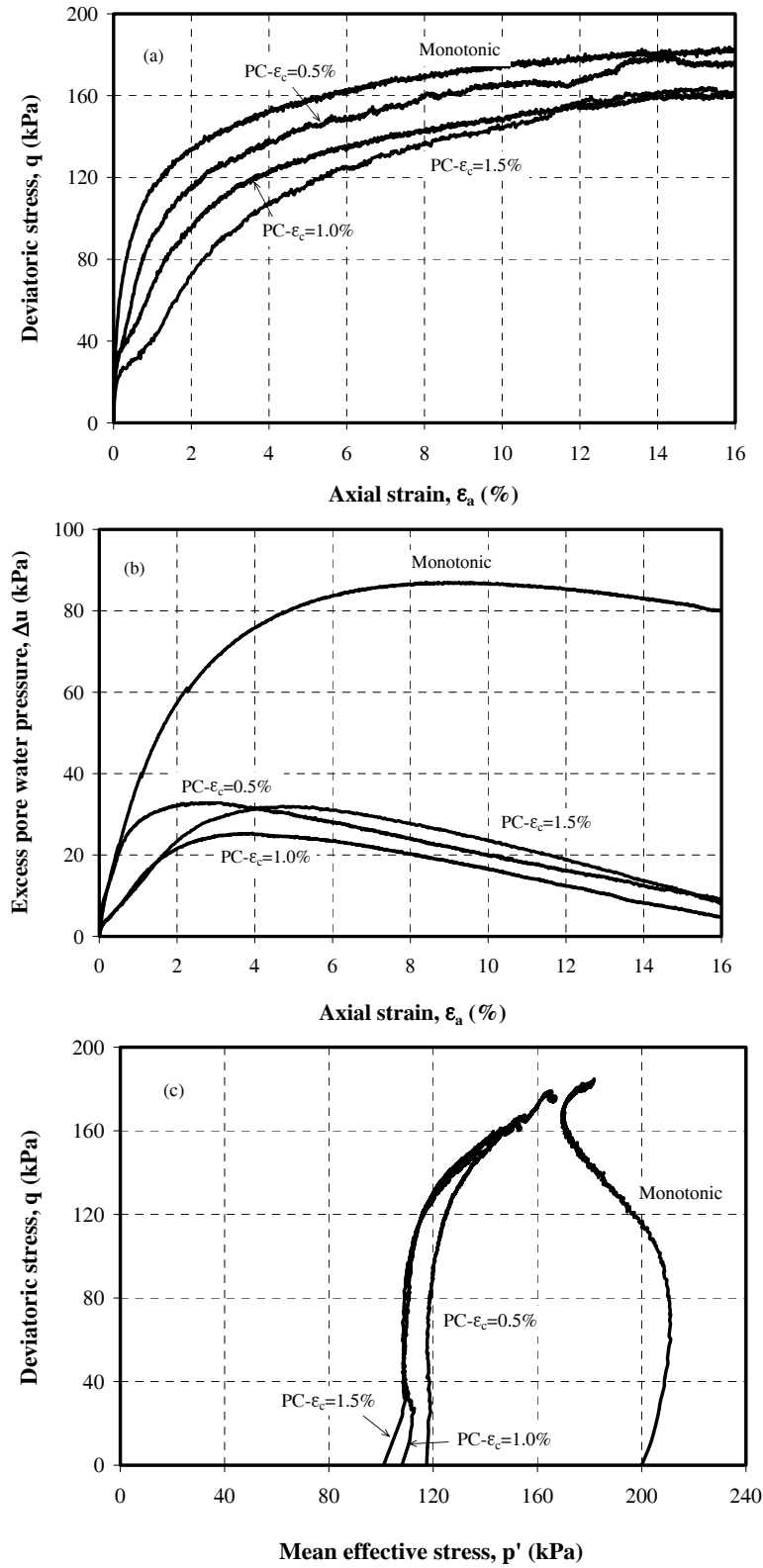


Figure 5. Effect of cyclic loading on post-cyclic behavior of specimen ST60 at  $\sigma'_c = 200$  kPa: a) deviatoric stress versus axial strain, b) excess pore water pressure versus axial strain and c) effective stress path

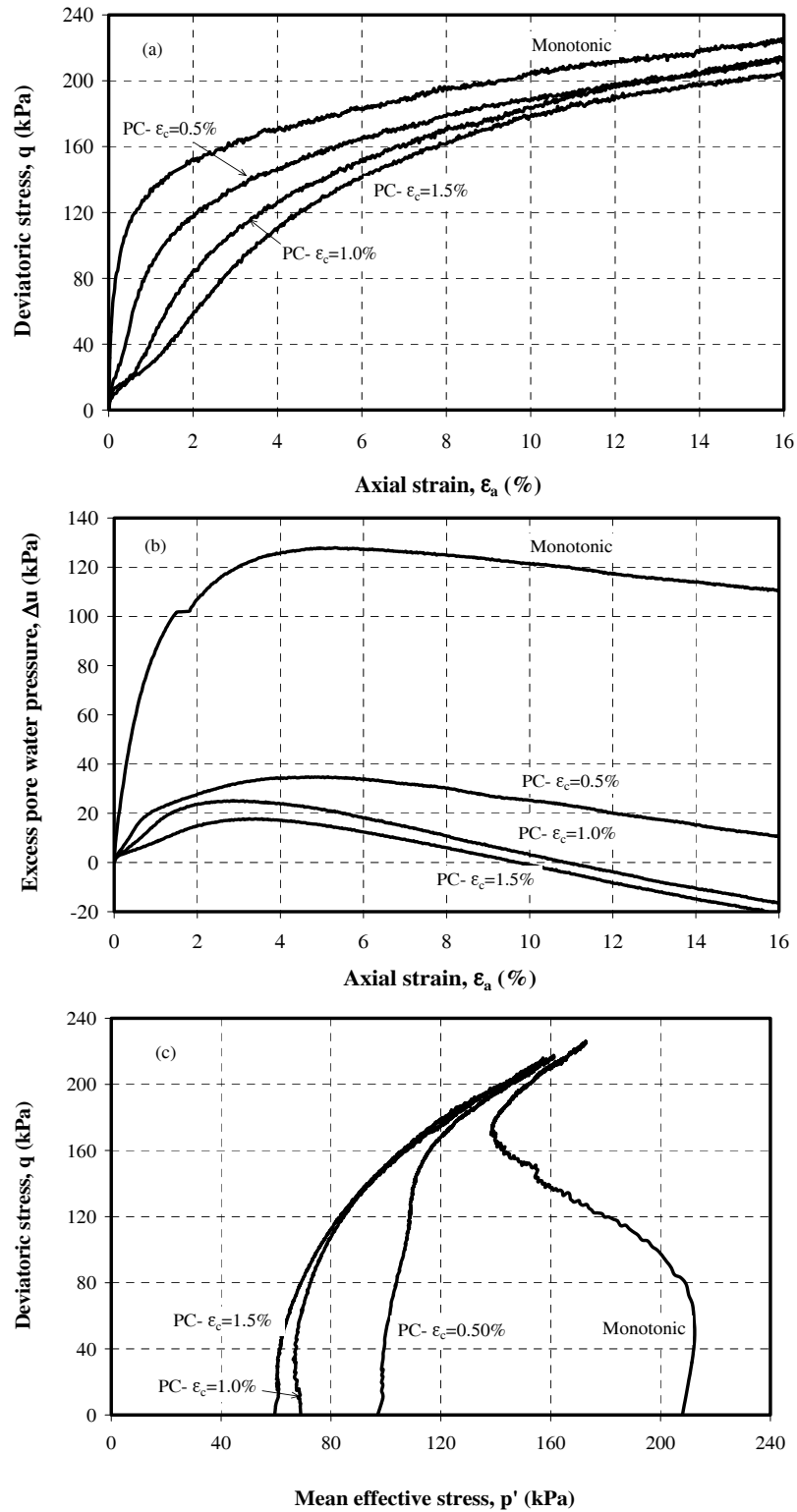


Figure 6. Effect of cyclic loading on post-cyclic behavior of specimen ST40 at  $\sigma'_c = 200$  kPa: a) deviatoric stress versus axial strain, b) excess pore water pressure versus axial strain and c) effective stress path



## 4. Analysis of Results

### 4.1. Effect of Cyclic Strain

#### 4.1.1. Stress-strain behavior

A comparison of the stress-strain behavior during the post-cyclic tests with the stress-strain behavior during the monotonic tests (examples presented in Figures 3a to 6a) suggests that the post-cyclic undrained shear strength and secant deformation modulus of the specimens are influenced by the cyclic loading and its amplitude. Variations of the normalized undrained shear strength ( $S_{uc(PC)}/S_{uc(M)}$ ) and normalized secant deformation modulus ( $E_{50(PC)}/E_{50(M)}$ ) versus the cyclic axial strain ( $\varepsilon_c$ ) for all of the tests are compiled in Figures 7 and 8, respectively. In these Figures, post-cyclic shear strength ( $S_{uc(PC)}$ ) and secant deformation modulus ( $E_{50(PC)}$ ) obtained from each of the tests have been normalized to their corresponding values resulted from the monotonic tests (Series I tests); it should be noted that  $\varepsilon_c=0$  represents the monotonic tests. In fact, the normalized values represent variations in the undrained shear strength and deformation modulus due to cyclic loading.

As observed in Figures 7 and 8, both of the normalized shear strength and normalized secant deformation modulus reduce as the cyclic axial strain,  $\varepsilon_c$ , increases. The degree of degradation of the deformation modulus is much higher than the degree of degradation of the shear strength. The behavior of the post-cyclic tests on specimens T100, which is pure clay, are in general agreement with the results of the similar tests reported in the literature [16, 17, 18 and 19]. For example, Matsui et al (1992) studied effect of cyclic axial strain on the post-cyclic behavior of two types of normally consolidated clay and concluded that in general the post-cyclic undrained shear strength and secant

deformation modulus of these clays decrease as cyclic axial strain increases. Also Yasuhara et al. (1992) investigated effect of undrained cyclic loading on clay behavior and found that the undrained shear strength decreases with the amplitude of cyclic loading. Moses et al. (2003) observed similar behavior for cemented clays.

There are a few exceptions in the shear strength of specimen T100, in which the post-cyclic test with  $\varepsilon_c=0.5\%$  reflects higher shear strength compared with the monotonic strength. The authors speculate that the reason for this anomaly in low cyclic strains may be due to either experimental error or reorientation of the clay flocks and particles (caused by cyclic loading) which results in a higher internal friction angle; the effect of friction (or strength) augmentation is dominant to the degradation caused by cyclic loading.

It should be noted that post-cyclic testing with the consolidation pressure ( $\sigma'_c$ ) of 100kPa, especially on the high-content sand specimens (ST60 and ST40), faced some difficulties because of very low confining pressures ( $p'_{pc}$ ) at the beginning of the post-cyclic tests. For example,  $p'_{pc}$  of the post-cyclic tests of these specimens with  $\varepsilon_c=0.5\%$  were 40.4 and 32.3kPa, respectively (Table 2). Therefore, our analyses and evaluation of the post-cyclic behavior of the soils hereafter will be mainly on the basis of the tests with  $\sigma'_c=200$  and 350kPa.

#### 4.1.2. Excess pore water pressure (EPWP)

In Figures 3b to 6b, one can observe that the excess pore water pressures (EPWPs) induced during the post-cyclic tests are significantly lower than EPWPs induced during the monotonic tests (Series I). Also the value of EPWP decreases as  $\varepsilon_c$  increases. It is of interest that the excess pore water

pressure behavior in the post-cyclic monotonic tests resembles the behavior of lightly overconsolidated soils.

In addition, the EPWPs in the post-cyclic tests as well as the monotonic tests increase initially during shearing, then after reaching a maximum value they follow a decreasing trend with increasing the axial strain. This reduction in EPWP is more pronounced in the post-cyclic tests, especially for the higher values of  $\varepsilon_c$ , with minimum values at the end of the tests. These minimum values are even negative for some of the tests with  $\varepsilon_c$  equal to 1.0% and 1.5% (See Figures 3b, 4b and 6b.).

#### 4.1.3. Effective stress path (q': p')

Figures 3c to 6c show the effective stress paths in q':p' planes for the tests with  $\sigma'_c=200\text{kPa}$ . It is observed that the post-cyclic stress paths start from comparatively lower values of p', and their behavior very much resembles the behavior of lightly overconsolidated soils. With reference to Table 2, the low values of mean effective stresses (p') at the beginning of the post-cyclic tests, as compared with their corresponding values at the beginning of the monotonic tests ( $\sigma'_c$ ), are caused by EPWPs induced during cyclic loading. Generally the higher the cyclic strain, the more the apparent overconsolidation ratio. Similar behavior was observed during the post-cyclic tests with  $\sigma'_c=100$  and 350kPa.

## 4.2. Effect of Sand Content

### 4.2.1. Stress-strain behavior

Variations of the normalized undrained shear strength and normalized secant deformation modulus versus the sand content for the values of  $\varepsilon_c$  are presented in Figures 9 and 10, respectively. It can be realized that with

the exception of two tests on T100 specimens (as discussed in Section 4.1.1), the undrained shear strength and secant deformation modulus of all of the specimens degraded due to cyclic loading. It is also realized that the degradation in the secant deformation modulus is comparatively more pronounced and more dependent on the sand content. For the mixed specimens, degradation in the shear strength and secant deformation modulus range respectively between 0.99 & 0.87, and 0.97 & 0.074.

### 4.2.2. Excess pore water pressure (EPWP)

Variations of the normalized maximum EPWPs ( $\Delta u_{max}/p'$ ) generated during the monotonic and corresponding post-cyclic tests versus the sand content are presented in Figure 11 for the different  $\varepsilon_c$ . In this Figure, the normalization is made to the effective confining stress (p') before shearing. Therefore, the values of p' for monotonic tests are their corresponding  $\sigma'_c$  and for the post-cyclic tests are the numbers summarized in Table 2. It can be observed that for the post-cyclic tests, with a few exceptions,  $\Delta u_{max}/p'$  increases mildly with the sand content. For the monotonic tests, the increase in  $\Delta u_{max}/p'$  with the sand content is more pronounced.

### 4.2.3. Effective stress path (q': p')

A review of Table 2 and Figures 3c to 6c suggests that for a given consolidation pressure ( $\sigma'_c$ ) and cyclic strain ( $\varepsilon_c$ ), the effective confining stresses (p') at the beginning of the post-cyclic shearing for most of the tests decreases as the sand content increases. This is a direct consequence of the fact that higher excess pore water pressures have been induced during cyclic loading in the tests on the specimens with the higher sand contents.

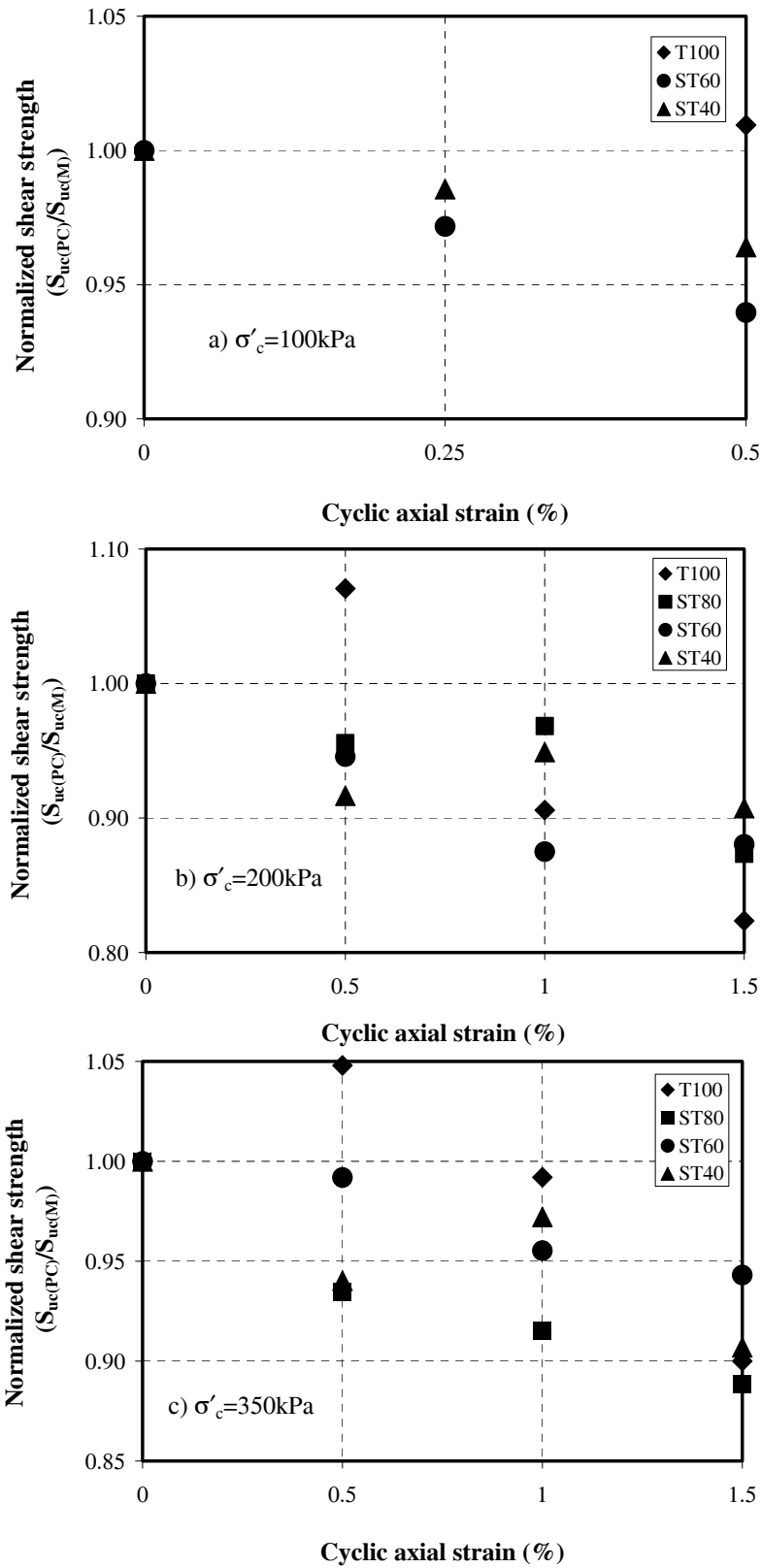


Figure 7. Variations of post-cyclic normalized undrained shear strength versus cyclic axial strain: a)  $\sigma'_c=100\text{kPa}$ , b)  $\sigma'_c=200\text{kPa}$  and c)  $\sigma'_c=350\text{kPa}$

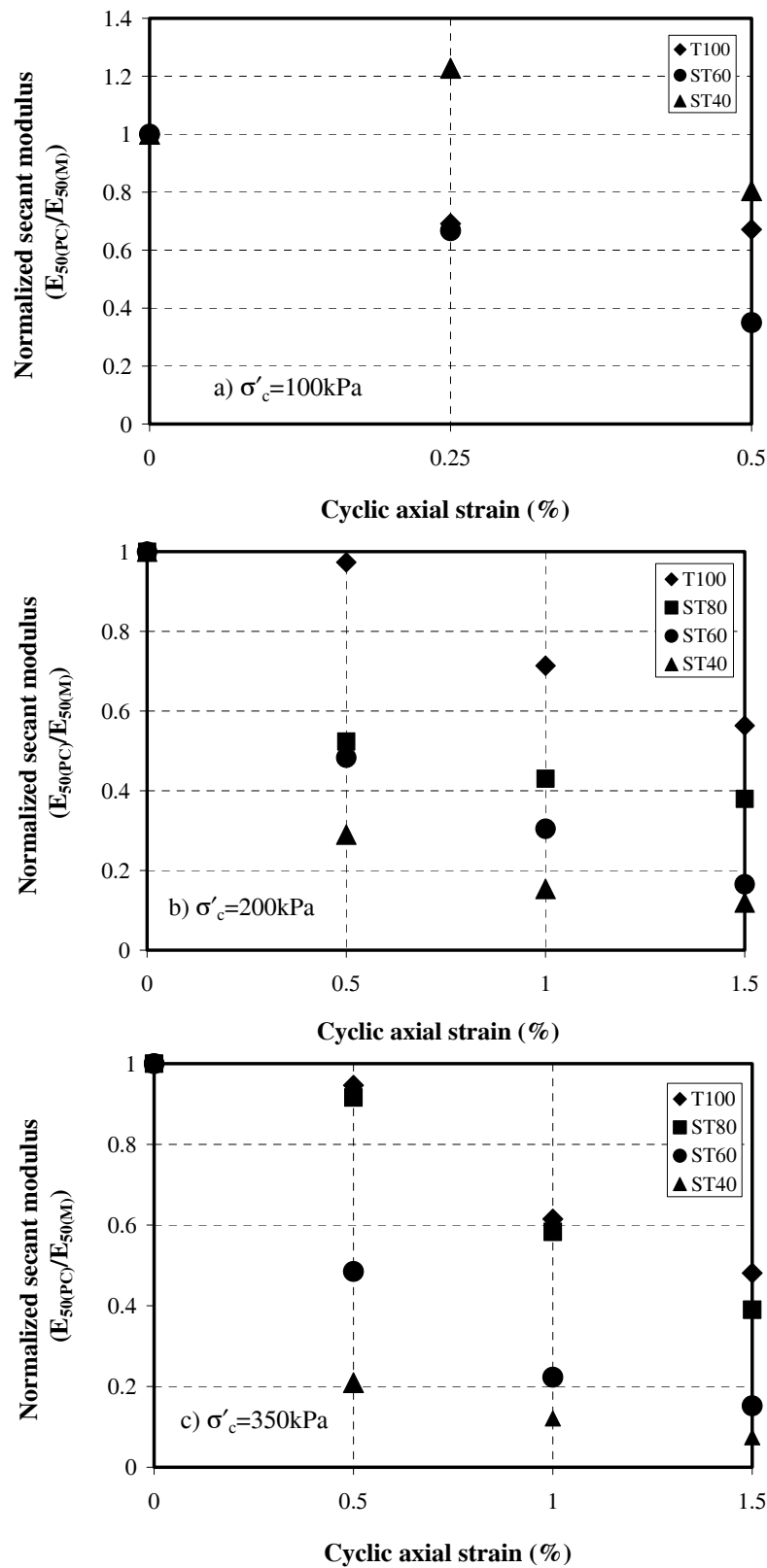


Figure 8. Variations of post-cyclic normalized secant modulus versus cyclic axial strain: a)  $\sigma'_c = 100\text{kPa}$ , b)  $\sigma'_c = 200\text{kPa}$  and c)  $\sigma'_c = 350\text{kPa}$

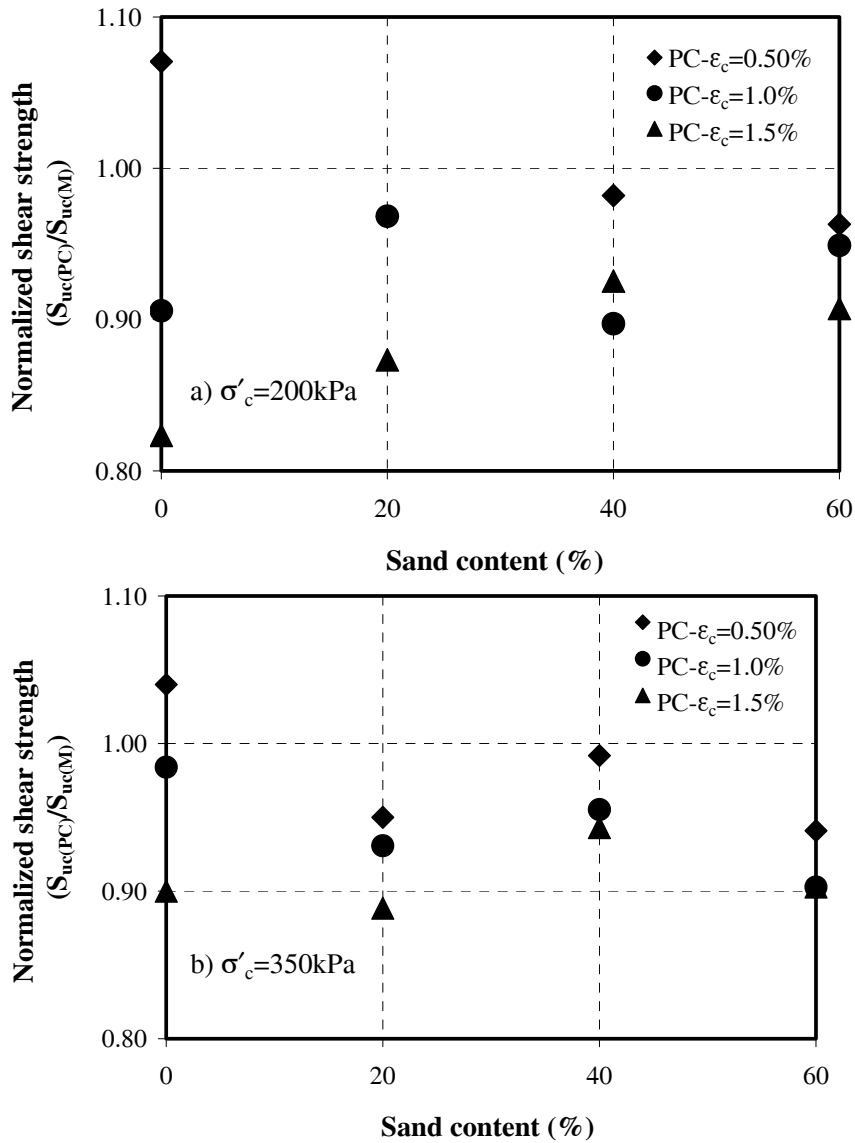


Figure 9. Variations of normalized undrained shear strength versus sand content for different cyclic strain at consolidation pressures of: a)  $\sigma'_c = 200 \text{ kPa}$  and b)  $\sigma'_c = 350 \text{ kPa}$

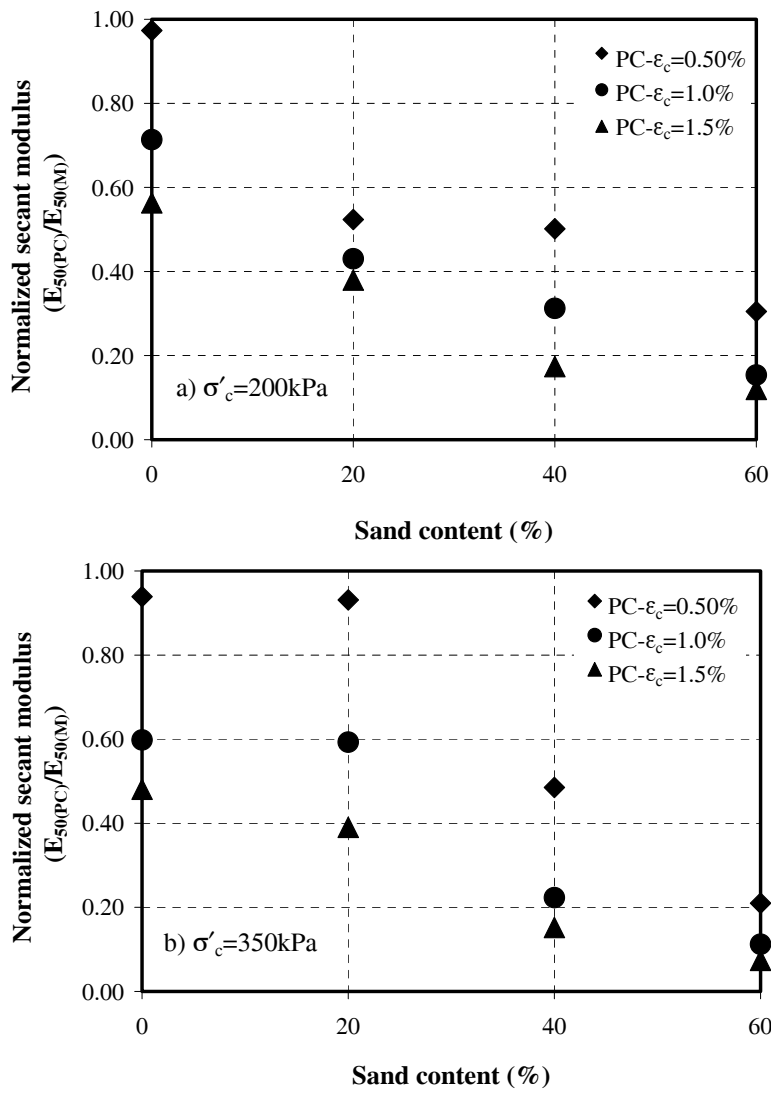


Figure 10. Variations of normalized secant deformation modulus versus sand content for different cyclic strain at consolidation pressures of: a)  $\sigma'_c=200\text{kPa}$  and b)  $\sigma'_c=350\text{kPa}$

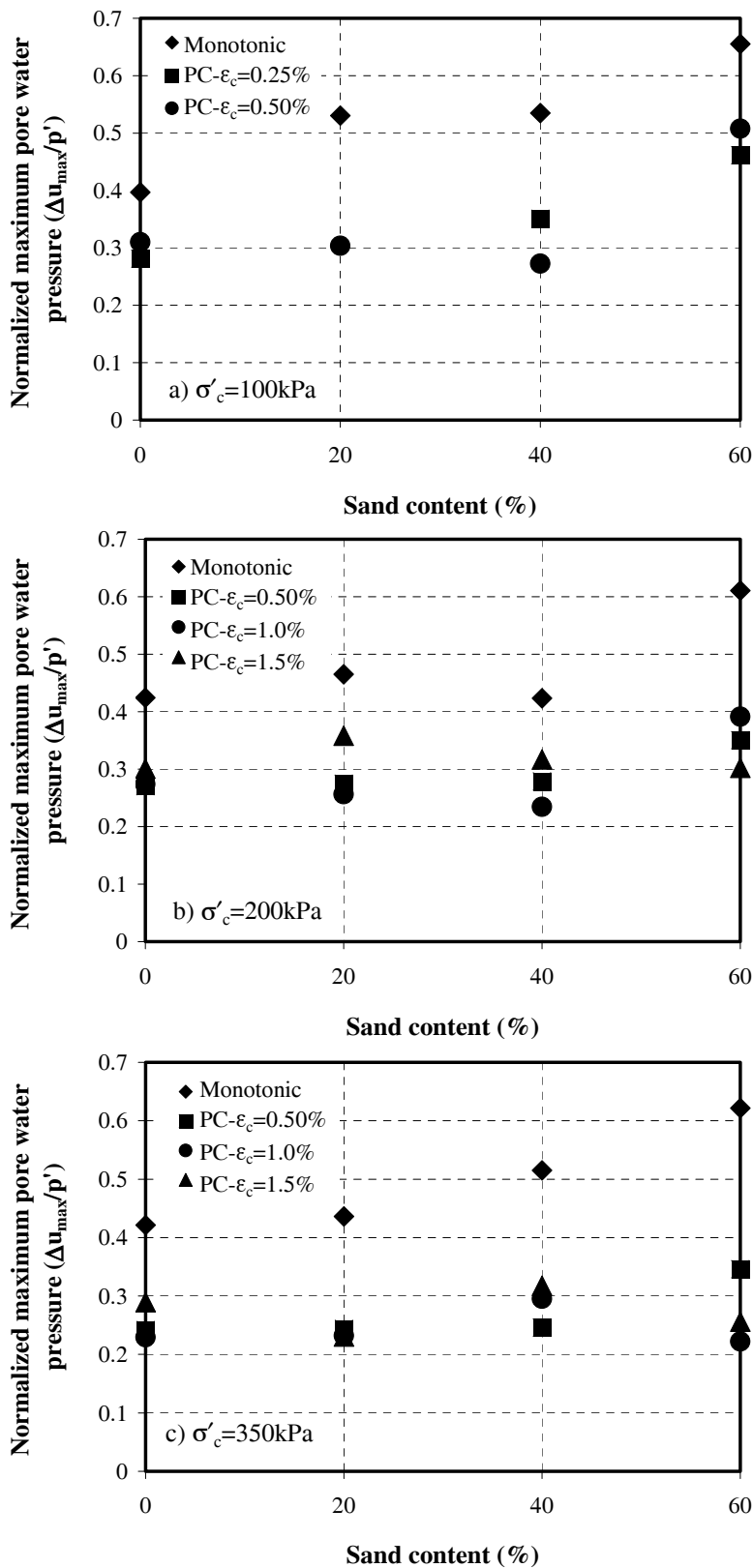


Figure 11. Variations of normalized maximum excess pore water pressure with sand content for different  $\epsilon_c$ :  
 a)  $\sigma'_c = 100 \text{ kPa}$ , b)  $\sigma'_c = 200 \text{ kPa}$  and c)  $\sigma'_c = 350 \text{ kPa}$

## 5. Summary and conclusions

The paper presents results of a number of consolidated undrained monotonic as well as post-cyclic triaxial compression tests on three sand-clay mixtures, with 20%, 40%, and 60% sand contents; three consolidation pressures of 100, 200, and 350kPa were used for testing. Similar tests were carried out on specimens of pure clay. On the basis of the tests results, the main conclusions of the paper are summarized, as follows:

- Undrained cyclic loading reduces effective stresses by generating excess pore water pressures and induces apparent overconsolidation in the specimens.

- The results of the post-cyclic monotonic tests show that cyclic loading degrades undrained shear strength and secant deformation modulus of the clay and mixed specimens.

- The degradation in mechanical properties depends on the sand content, cyclic axial strain level, and to some degrees confining pressure.

- The values of excess pore water pressures developed during the post-cyclic tests are considerably lower than the associated values developed during the monotonic tests.

- The conclusions and results presented in this paper may be adopted for the evaluation of mechanical parameters required for post-earthquake stress-strain and stability analyses of soil structures comprising clay or clay-granular material mixtures.

### Notation

$E_{50(M)}$  = Secant deformation modulus obtained from monotonic test

$E_{50(PC)}$  = Secant deformation modulus obtained from post-cyclic monotonic test

**EPWP** = Excess Pore Water Pressure

$G_S$  = Specific gravity

**LL** = Liquid limit

**OCR<sub>app</sub>** = Apparent overconsolidation ratio

**PI** = Plasticity index

$p'$  = Mean effective stress

$p'_{pc}$  = Mean effective stress at the beginning of post-cyclic monotonic shearing

$q$  = Deviatoric stress

$S_{uc(M)}$  = Undrained shear strength obtained from monotonic test

$S_{uc(PC)}$  = Undrained shear strength obtained from post-cyclic monotonic test

$w$  = Water content

$\Delta u_{max}$  = Maximum excess pore water pressures

$\gamma_d$  = Dry density

$\varepsilon_a$  = Axial strain

$\varepsilon_c$  = Cyclic axial strain

$\sigma'_c$  = Consolidation pressure

### References

- [1] Nakase, A., Nakanodo, H. and Kusakabe, O. "Influence of soil type on pore pressure response to cyclic loading", Proc. 5<sup>th</sup> Japan Earthquake Engrg. Symp. pp 593-600 (1978).
- [2] Nakase, A. and Kamei, T. "Undrained shear strength anisotropy of normally consolidated cohesive soils", Soils and Founds., 23(1), pp 91-101 (1983).
- [3] Kimura, T., Takemura, J., Hiro-Oka, A., and Okamura, M. "Mechanical behavior of intermediate soils", Proc. of In.Conf. Centrifuge, A.A. Balkema, Rotterdam, (1994).
- [4] Bayoglu, E. "Shear strength and compressibility behavior of sand-clay mixtures", M.Sc. thesis, Department of



- Civil Engineering, Middle-East Technical University, Ankara, Turkey, (1995).
- [5] Kuwano, J., Imura, H., Takahara, K., and Nakagawa, H. "Undrained cyclic and monotonic shear behavior of sand-kaolin mixed", First Int. Conf. on Earthquake Geotech. Engrg, A.A. Balkema, Rotterdam, 1, pp 165-170 (1995).
- [6] Vallejo, L. E., and Mawby, R. "Void ratio influence on the shear strength of granular material-clay mixtures", *Engrg Geology*, 58, pp 125-136 (2000).
- [7] El-Mesmary, M.A., Nabeshima, Y., and Matsui, T. "Influence of clay content and clay type on cyclic behavior of compacted intermediate soils", Proc. 11<sup>th</sup> Int. Offshore and Polar Engrg Conf., Stavanger, Narway, June17-22, II, pp 512-517 (2001).
- [8] Jafari, M.K. and Shafiee, A. "Mechanical behavior of compacted composite clays", *Can. Geotech J.*, 41, pp 1152-1167 (2004).
- [9] Ambraseys, N. N., and Sarma, S. K. "Liquefaction of soils induced by earthquake", *Bull. Seismol. Soc. Am.*, 59 (2), pp 651-664 (1969).
- [10] Seed, H.B. "Nineteenth Rankin lecture: Consideration in the earthquake resistance design of earth and rockfill dam", *Geotechnique*, 29, London, England, pp 215-263 (1979).
- [11] Ishihara, K. "Post-earthquake failure of a tailings dam due to liquefaction of the pond deposit", Int. Conf. on Case Histories in Geotech. Engrg., St. Louis, 3, pp 1129-1143 (1984).
- [12] Ishihara, K., Verdugo, R., and Acacio, A. A. "Characterization of cyclic behavior of sand and post-seismic analyses", Proc. of the Ninth Asian Regional Conf. on Soil Mech. and Found. Engrg., Bangkok, Thailand , 2, pp 45-68 (1991).
- [13] Gu, W.H., Morgenstern, N.R. and Robertson, P.K. "Progressive failure of Lower San Fernando Dam", *J.of Geotech.Engrg.*, 119(1), pp 333-348 (1993).
- [14] Pillai, V.S. and Salgado, F.M. "Post-liquefaction stability and deformation analysis of Duncan Dam", *Can. Geotech. J.*, 31(6), pp 967-978 (1994).
- [15] Soroush, A., Morgenstern, N.R., Robertson, P.K. and Chan, D. "The earthquake deformation analysis of the Upper San Fernando Dam", Proc. of Int. Symp on Seismic and Environ. Aspects of Dams, 1, pp 405-418 (1996).
- [16] Matsui, T., Bahr, M. A., and Abe, N. "Estimation of shear characteristics degradation and stress-strain relation of saturated clays after cyclic loading", *Soils and Founds*, 32(1), pp 161-172 (1992).
- [17] Yasuhara, K., Hiro., K., and Hyde, A.F.L. "Effects of cyclic loading on strength and compressibility of clays", *Soils and Founds.*, 32(1), pp 100-116 (1992).
- [18] Jitno,H. and Vaid, Y.P. "Post-cyclic Monotonic Behavior of a Marine Clay", Proc. Ninth Asian Regional

- Conf., Bangkok, Thailand, 1, pp 41-44 (1991).
- [19] Moses, G.G., Rao, S.N., and Rao, P.N. "Undrained strength behavior of a cemented marine clay under monotonic and cyclic loading", *Ocean Engrg.*, 30, pp 1765-1789 (2003).
- [20] Yasuhara, K. "Post-cyclic degradation and recovery in undrained strength of clays", *Performance of Ground and Soil Structures during earthquakes*, 13<sup>th</sup> ICSMFE, New Dehli, pp 93-108 (1994).
- [21] Olivers, L., and Silvestri, F. "Observation on the pre- and post-cyclic compression and stiffness properties of a reconstituted high plasticity clay", *Compression and Consolidation of Clayey Soils*, Yoshikuni and Kasakabe, Balkema, Rotterdam, pp 155-160 (1995).
- [22] Seed, H.B., Martin, P.P. and Lysmer, J. "Pore-water pressure change during soil liquefaction", *J. of Soil Mech. and Found. Div., ASCE*, 102(GT4), pp 323-346 (1976).
- [23] Vaid, Y. P., Thomas, J. "Liquefaction and post-liquefaction behavior of sand", *J. of Geotech. Engrg.*, 121(2), pp 163-173 (1995).
- [24] Olson, S.M. and Stark, T.D. "CPT Based Liquefaction Resistance and Post-Liquefaction Shear Strength", *Specialty Conf. on Geotech. Earthquake Engrg. and Soil Dynamics*, University of Illinois, Urbana-Champaign, August 3-6, Washington, USA, (1998).
- [25] Song, B.-W. "The influence of initial static shear stress on post-cyclic degradation of non-plastic silt", *Lowland Tech. Int., Int. Assoc. of Lowland Tech.*, ISSN 1344-9656, 4(2), pp 14-24 (2002).
- [26] Sivathayalan, S. and Mehrabi Yazdi, A. "Post liquefaction response of initially strain softening sand", *Int. Conf. on Cyclic Behavior of Soils and Liquefaction Phenomena Bochum, Germany*, 31 March – 02 April, (2004).
- [27] Yasuhara, K., Murakami, S., Song, B. W., Yokokawa, S. and Hyde, A. F. L. "Post-cyclic Degradation of Strength and Stiffness for Low Plasticity Silt", *J. of Geotech. and Geoenviron. Engrg.*, 129(8), pp 756-769 (2003).
- [28] Yasuhara, K., Hyde, A.F.L. and Murakami, S. "Post-cyclic degradation of saturated plasticity silts", *Int. Conf. on Cyclic Behavior of Soils and Liquefaction Phenomena Bochum, Germany*, 31 March – 02 April, (2004).
- [29] *Annual Book of ASTM Standards*, Vol: 04.08 (1997).
- [30] Matasovic, N., and Vucetic, M. "A Pore Pressure Model for Cyclic Straining of Clay", *Soils and Found.*, 32(3), pp 156-173 (1992).